Speaker-normalized vowel representations in the human auditory cortex

Matthias J. Sjerps[1,2], Neal P. Fox[3], Keith Johnson[4], Edward F. Chang*[3,5,6]

[1] Donders Institute for Brain, Cognition and Behaviour, Centre for Cognition, Radboud University, Nijmegen, The Netherlands

[2] Max Planck Institute for Psycholinguistics, Nijmegen, The Netherlands

[3] Department of Neurological Surgery, University of California, San Francisco, CA, USA

[4] Department of Linguistics, University of California, Berkeley, CA, USA

[5] Center for Integrative Neuroscience, University of California, San Francisco, CA, USA

[6] Department of Physiology, University of California, San Francisco

*Corresponding author. Email: edward.chang@ucsf.edu

Short title: Speaker normalization in human cortex

Abstract

Humans identify speech sounds, the fundamental building blocks of spoken language, using the same cues, or acoustic dimensions, as those that differentiate the voices of different speakers. The correct interpretation of speech cues is hence uncertain, and requires normalizing to the specific speaker. Here we assess how the human brain uses speaker-related contextual information to constrain the processing of speech cues. Using high-density electrocorticography, we recorded local neural activity from the cortical surface of participants who were engaged in a speech sound identification task. The speech sounds were preceded by speech from different speakers whose voices differed along the same acoustic dimension that differentiated the target speech sounds (the first formant; the lowest resonance frequency of the vocal tract). We found that the same acoustic speech sound tokens were perceived differently, and evoked different neural responses in auditory cortex, when they were heard in the context of different speakers. Such normalization involved the rescaling of acoustic-phonetic representations of speech, demonstrating a form of recoding before the signal is mapped onto phonemes or higher level linguistic units. This process is the result of auditory cortex' sensitivity to the contrast between the dominant frequencies in speech sounds and those in their just preceding context. These findings provide important insights into the mechanistic implementation of normalization in human listeners. Moreover, they provide the first direct evidence of speaker-normalized speech sound representations in human parabelt auditory cortex, highlighting its critical role in resolving variability in sensory signals.

Introduction

A fundamental computational challenge faced by perceptual systems is the lack of a one-to-one mapping between highly variable sensory signals and the discrete, behaviorally relevant events they reflect[1,2]. A profound example of this problem exists in human speech perception, where the main cues to speech sound identity are the same as those to speaker identity[3–5].

For example, to distinguish a given speaker's /*u*/ from his or her /*o*/ (distinguishing "boot" from "boat"), listeners rely heavily on the vowel's first formant frequency (F1; the first vocal tract resonance) because it is lower for /u/ than for /o/[6]. However, people with long vocal tracts (typically tall male speakers) have overall lower resonance frequencies than those of speakers with shorter vocal tracts. Consequently, a tall person's production of the word "boat" and a short person's "boot" might be acoustically identical. Behavioral research has suggested that preceding context allows listeners to "tune-in" to the acoustic properties of a particular voice and *normalize* subsequent speech input[7–11]. The most well-known example of this effect is that a single acoustic token, ambiguous between /u/ and /o/, will be labelled as /o/ after a context sentence spoken by a tall-sounding person (low F1), but like /u/ after a context sentence spoken by a shorter-sounding person (high F1)[12].

The neurobiological foundations of context-based speaker normalization remain largely unknown. Neural activity in auditory cortex is sensitive to acoustic cues that are critical for both recognizing and discriminating phonemes[13–19] and different talkers[20–24]. For example, recent work has shown that speech sound representations in STG are closely related to the acoustic-phonetic features that define classes of speech sounds, like F1. Vowels with low F1 frequencies (e.g., /u/, /i/) can be distinguished from vowels with relatively higher F1 frequencies (e.g., /o/, /æ/) based on local activity on STG[25]. A critical question that arises, then, is whether the feature-based representations in auditory cortex are normalized (i.e., feature rescaling), or whether they continue to closely reflect the veridical acoustic properties of the input.

To investigate the influence of context on auditory cortex speech sound representations, we recorded cortical local field potentials with subdurally implanted high density electrode arrays that covered the broader peri-sylvian language region in human participants while they listened to and identified vowel sounds presented in the context of sentences spoken by two different voices[14,26]. We found direct evidence of speaker-normalized neural representations of vowel sounds in parabelt auditory cortex, including superior and middle temporal gyri. Normalization was observed in populations that were selective for acoustic-phonetic (i.e., pre-phonemic) properties of the speech signal. These effects were at least partly driven by the contrastive relation between the F1 range in the context sentences and F1 values in the target vowels. More generally, the results demonstrate the critical role of human auditory cortex in integrating incoming sounds with surrounding acoustic context.

Results

We recorded neural activity directly from the cortical surface of five Spanish-speaking neurosurgical patients while they voluntarily participated in a speech sound identification task. They listened to Spanish sentences that ended in a (pseudoword) target, which they categorized as either “sufu” or “sofo” on each trial with a button press (Figure 1a, b). The sentence-final targets comprised a digitally synthesized six-step continuum morphing from an unambiguous *sufu* to an unambiguous *sofo*, with four intermediate tokens (*s?f?*, i.e., spanning a perceptually ambiguous range). On each trial, a pseudo-randomly selected target was preceded by a context sentence (*A veces se halla…*; “*At times she feels rather…*”). Two versions of this context sentence were synthesized, differing only in their mean F1 frequencies (Figure 1a, c; Figure S1), yielding two contexts that listeners perceive as consistent with two speakers: one with a long vocal tract (low F1; Speaker A) and one with a short vocal tract (high F1; Speaker B). Critically, F1 frequency is the primary acoustic dimension that distinguishes between the vowels /*u*/ and /*o*/ in natural speech (in both Spanish and English), as well as in our target

73 continuum (Figure 1a and Figure S1)[6]. Similar materials have previously been shown to
74 induce a reliable shift in the perception of an /u/ – /o/ continuum (a “normalization effect”) in
75 healthy Spanish-, English-, and Dutch-listeners[8].

76 As expected, participants’ perception of the target continuum was affected by the F1
77 range of the preceding sentence context ($p < 0.002$; Figure 1d). Specifically, participants were
78 more likely to identify tokens as *sofo* (the vowel category corresponding to higher F1 values)
79 after a low F1 voice (Speaker A) compared to the same target presented after a high F1 voice
80 (Speaker B). Hence, listeners’ perceptual boundary between the /*u*/ and /*o*/ vowel categories
81 shifted to more closely reflect the F1 range of the context speaker. Past work has interpreted
82 this classical finding in light of the contrastive perceptual effects that are ubiquitous among
83 sensory systems[27]: the F1 of a speech target will sound relatively higher (i.e., sound more like
84 an /o/) after a low F1 context sentence than after a high F1 context. This results in a shift of the
85 category boundary to lower F1 values.
86

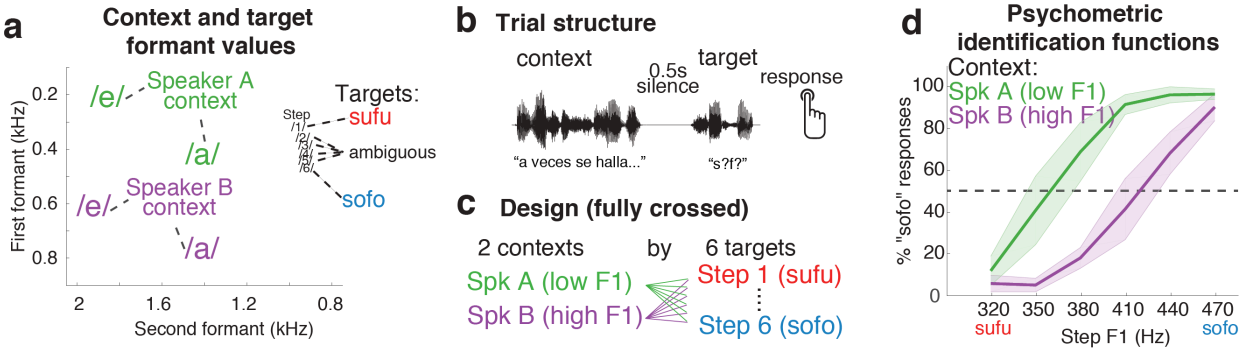

87

88 *Figure 1:* ***Listeners perceive speech sounds relative to their acoustic context. a****) Target*
89 *sounds were synthesized to create a 6 step continuum ranging from /sufu/ (step 1; low first*
90 *formant [F1]) to /sofo/ (step 6; high F1). Context sentences were synthesized to sound like two*
91 *different speakers: a speaker with a long vocal tract (low F1 range: Speaker A), and a speaker*
92 *with a short vocal tract (high F1 range; Speaker B). Context sentences contained only the*
93 *vowels /e/ and /a/, but not the target vowels /u/ and /o/. Following phonetic convention, the*

formant axes are reversed (higher values at the bottom/left sides of the panel). ***b****) Context sentences preceded the target on each trial (separated by 0.5 seconds of silence), after which participants responded with a button press to indicate whether they heard "sufu" or "sofo".* ***c****) All targets were presented after both speaker contexts.* ***d****) Listeners more often gave "sofo" responses to target sounds if the preceding context was spoken by Speaker A (low F1) than Speaker B (high F1).*

Human auditory cortex exhibits context-dependent speech sound representations. Two of the most influential hypotheses explaining the phenomenon of speaker normalization posit that: 1) contrast enhancing processes, operating at general auditory processing levels, change the representation of the input signal before it is mapped onto phonemes or higher level linguistic units[28–30]; 2) alternatively, it has been suggested that auditory processing of speech cues remains mostly faithful to the acoustics of the input signal, and normalization is a consequence of speaker-specific mapping of the veridical acoustics onto meaningful units (i.e., listeners have learned to associate an F1 of 400Hz to /u/-words for speakers, or vocal tract, that sound short, but to /o/-words for ones that sound taller)[9,31].

Past neurobiological work has demonstrated that neural populations in the parabelt auditory cortex are sensitive to acoustic-phonetic cues that distinguish classes of speech sounds, including vowels, and not to specific phonemes per se[25]. Hence, the primary goal of the current study was to examine whether the F1 range in preceding context sentences influence the representation of speech sounds in parabelt (nonprimary) auditory cortex in a normalizing way. We investigated whether the neural representation of vowel stimuli remains veridical (i.e., unaffected by context) or, alternatively, whether it becomes shifted towards the representation typical of /u/ in the context of a high F1 speaker, but towards /o/ in the context of a low F1 speaker. We first tested whether individual cortical sites that reliably differentiate between vowels (i.e., discriminate /u/ from /o/ in their neural response) would exhibit

120 normalization effects. A secondary goal of the current study was to confirm that the response
121 profile of those cortical populations that display normalization was indeed acoustic-phonetic
122 (i.e., pre-phonemic) in nature. We therefore assessed populations' responsiveness during the
123 context sentences as well (context sentences did not contain the target phonemes /o/ and /u/
124 but did traverse the same acoustic F1 region).

125 To this end, we extracted the stimulus-aligned analytic amplitude of the high-gamma
126 band (70-150 Hz) of the local field potential at each temporal lobe electrode (n = 406 across
127 patients; this number is used for all Bonferroni corrections below) during each trial. High-gamma
128 activity is a spatially- and temporally-resolved neural signal that has been shown to reliably
129 encode phonetic properties of speech sounds[25,32,33], and is correlated with local neuronal
130 spiking[34–36]. We used general linear regression models to identify cortical patches involved in
131 the representation of context and/or target acoustics. Specifically, we examined the extent to
132 which high-gamma activity at each electrode depended on stimulus conditions during
133 presentation of the context sentences (context window) or during presentation of the target
134 (target window; see supplemental materials). The fully specified encoding models included
135 numerical variables for the target vowel F1 (Steps 1-6) and context F1 (high vs. low), as well as
136 their interaction. In the following, we focused on "task-related electrodes", defined as the subset
137 of temporal lobe electrodes for which a significant portion of the variance was explained by the
138 full model, either during the target window or the during context window ($p < 0.05$; uncorrected,
139 n = 98; see Figure S2).

140 Among the task-related electrodes, some displayed selectivity to target vowel F1 (Figure
141 2a). Consistent with previous reports of auditory cortex tuning for vowels[25] we observed that
142 different subsets of electrodes displayed a preference for either "sufu" or "sofo" targets (color
143 coded in Figure 2a). Figure 2b and Figure 2c (middle panel) display the response profile for one
144 example electrode that had a "sofo" preference (e1; $p = 6.8*10^{-19}$). Importantly, in addition to an
145 overall selectivity to the target sound F1, the activation level of this electrode was modulated by

146 the F1 range of the *preceding* context (Figure 2b & bottom panel of Figure 2c; $p = 5.8*10^{-6}$). This
147 demonstrates that the responsiveness of a neural population that is sensitive to bottom-up
148 acoustic cues is also affected by the distribution of that cue in preceding context. The direction
149 of this influence is analogous to the behavioral normalization effect.

150 To quantify this normalization effect across all electrodes that display selectivity to target
151 acoustics, we calculated the correlation between electrodes' *target preference* (numerically
152 defined as the glm-based signed t-statistic of the target F1 factor during the target window) and
153 their *context effect* (defined as the t-statistic of the context F1 factor during the target window).
154 We found a correlation between electrodes' target preferences and context effects (Figure 2d).
155 Crucially, this strong relationship had a negative slope, such that electrodes that had high-F1
156 target preferences (sofo > sufu) had stronger responses to targets after low F1 context
157 sentences (low F1 context > high F1 context; $r = -0.65$; $p = 1.3*10^{-6}$). Importantly, this
158 demonstrates that the relationship between context response and target response reflects an
159 encoding of the contrast between the formant properties of each, recapitulating the
160 normalization pattern observed in the behavioral responses (Fig 1d).
161

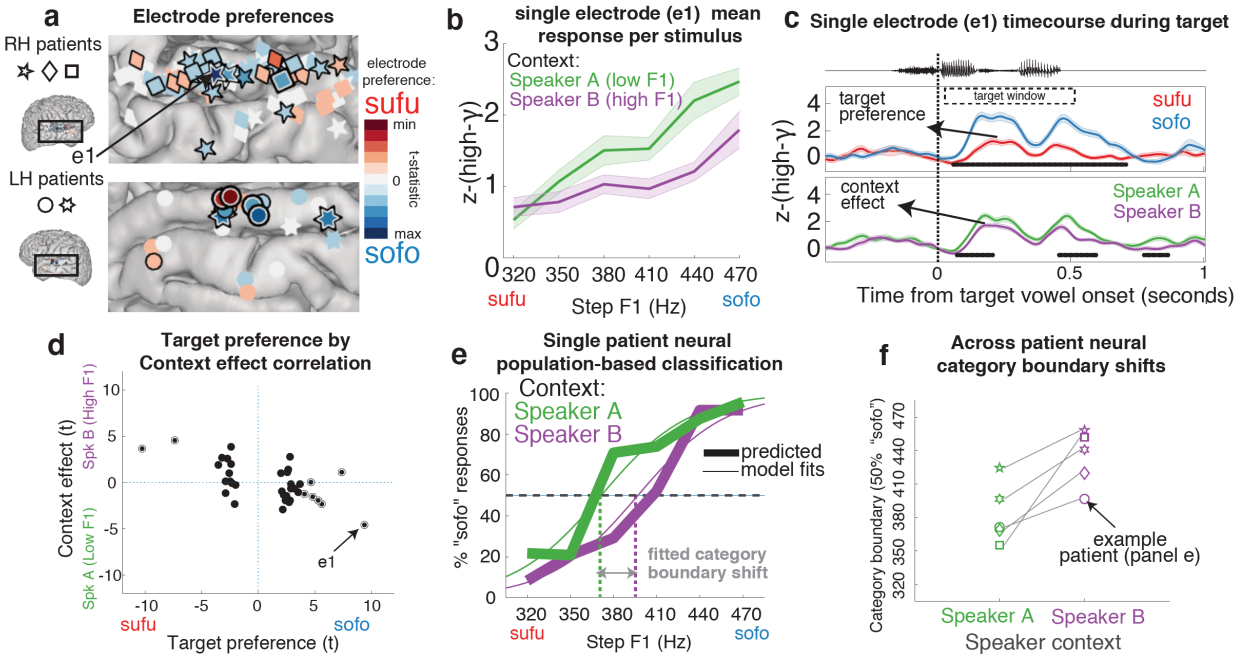

Figure 2: ***The neural response to bottom-up acoustic input is modulated by preceding context****.* ***a****) Target vowel preferences and locations (plotted on an MNI brain) for electrodes from all patients (3 with right hemisphere [RH] and 2 with left hemisphere [LH] grid implants). Only those temporal lobe electrodes where the full omnibus model was significant during the context and/or the target window (F-test; p<0.05) are displayed. Strong target F1 selectivity is relatively uncommon: electrodes with a black-and-white outline are significant at Bonferroni corrected p<0.05 (n = 9, out of 406 temporal lobe electrodes); a single black outline indicates significance at only p<0.05, uncorrected (n = 28). Activity from the indicated electrode (e1) is shown in b and c.* ***b****). Example of normalization in a single electrode (e1; z-scored high-gamma [high-γ] response averaged across the target window [target window marked in c]; +-1SE).* ***c****) Activity from e1 across time, separating the endpoint targets (top panel) or the contexts (bottom panel). The electrode responds more strongly to /o/ stimuli than /u/ stimuli, but also responds more strongly overall after Speaker A (low F1). This effect is analogous to the behavioral normalization (Fig. 1d). Black bars at the bottom of the panels indicate significant time-clusters (cluster-based permutation test of significance).* ***d****) Among all electrodes with significant target*

sound selectivity (n = 37 [9 + 28]), a relation exists between the by-electrode context effect and target preference. Both are expressed as a signed t-value, demonstrating that the size and direction of the target preferences predicts the size and direction of the context effects. As per a, symbol style reflects level of significance (solid back = p<0.05 uncorrected; black-and-white = p<0.05 Bonferroni corrected). ***e)*** *An LDA classifier was trained on the distributed neural responses elicited by the "sufu" and "sofo" stimuli using all endpoint selective electrodes of a patient. This model was then used to predict classes for (held-out) endpoint data and for the ambiguous steps. Proportions of neurally-based "sofo" predicted trials (thick lines) display a relative shift between the two context conditions (data from one example patient). Regression lines were fitted to these data for each participant separately to estimate 50% category boundaries per condition for panel f (thin lines).* ***f)*** *The neural classification functions display a shift in category boundaries between context conditions for all patients individually. Symbols denote individual participants.*

Normalization of distributed vowel representations in all participants. Figure 2d demonstrates that local populations in auditory cortex that are selective to target vowel F1 exhibit normalization. However, only a few electrodes (n = 9, out of 406 temporal lobe electrodes) displayed very strong target vowel selectivity (significance at Bonferroni-corrected p <0.05), while the majority of target F1 selective electrodes displayed only moderate selectivity and context effects. Moreover, not all participants had such highly target F1 selective electrodes (see Table S2). The relative sparseness of strong selectivity is not surprising given that the target vowel synthesis involved only small F1 frequency differences (~30Hz) per step, with the endpoints being separated by only 150Hz (which is, however, a prototypical F1 distance between /u/ and /o/[8]). However, past work has demonstrated that even small acoustic differences among speech sounds are robustly encoded by distributed patterns of neural activity across auditory cortex[14,37]. In order to determine whether distributed neural representations

of vowels reliably display normalization across all participants, we trained a multivariate pattern classifier model (Linear Discriminant Analysis, LDA) on the spatiotemporal neural response patterns of each participant. Models were trained to discriminate between the endpoint stimuli (i.e., trained on the neural responses to steps 1 vs. 6, irrespective of context) using all task-related electrodes for that participant. These models were then used to predict labels for held-out data of both the endpoints and the ambiguous steps. For all participants, classification of held-out endpoint trials was significantly better than chance (Figure S3b). To assess the influence of target F1 and context F1 on the classifier output, a logistic generalized linear mixed model was then fit to the proportion of predicted "sofo" responses across all participants.

Figure 2e displays the proportion of "sofo" labels predicted for all stimuli by the LDA classifier based on the neural data of one example participant (thick lines). Importantly, a shift is observed in the point of crossing of the category boundary. Regression functions fitted to these data (thin lines) allowed us to estimate the size and direction of the context-driven neural boundary (50% crossover point) shift per participant. For all participants, the neural vowel boundaries were found to be context dependent (Figure 2f; see online methods and Supplementary Figure S3 for further detail). The combined regression analysis demonstrated that, across participants, population neural activity in the temporal lobe was modulated both by the acoustic properties of the target vowel ($p = 1.2*10^{-7}$) and by the preceding context ($p = 4.2*10^{-8}$). This effect was not dependent on the approach to exclusively train on endpoint data (Figure S5). Moreover, this effect was not observed for task-related electrodes outside of the temporal lobe during the target window (see S4; non-temporal electrodes were mostly located on sensorimotor cortex and the inferior frontal gyrus).

Importantly, and in analogy to the behavioral results, the neural classification functions demonstrate that the influence of the context sentences consistently affected target vowel representations in a normalizing direction: the neural response of a target vowel with a given F1

is more like that of /o/ (high F1), after a low F1 context (Speaker A) than after a high F1 context (Speaker B; see Supplementary Figure S3 and S4b for more detail).

Normalization as sensitivity to contrast in acoustic-phonetic features. It has been suggested that a major organizing principle of human parabelt auditory cortex concerns the acoustic phonetic features that define classes of speech sounds, and not phonemes (or even higher level linguistic representations) per se[13,25,38]. Here we demonstrated normalization in these representations. However, auditory cortex processing is diverse and may contain regions that are in fact selective for (more abstract) phonemes. For example, auditory cortex has been found to display properties that are typically associated with abstract sound categories such as categorical perception, too[14]. Hence, we next assessed whether the normalization effects observed here involved a rescaling in patches of cortex that display sensitivity to acoustic-phonetic features (i.e., relating to more general F1 characteristics) or, instead, only in those patches that may be selective for discrete phonemes (or the target words as a whole). Because the context sentence did not contain the target vowels /u/ or /o/, but did traverse the same general F1 range, assessing electrodes' responses during the context window could inform us about the nature of their preferences.

To this end we again relied on the glm-based t-statistics of all target selective temporal lobe electrodes (n = 37; as per Figure 2d). Among these electrodes, however, we examined the relationship between their preferences for context F1 during the context window and for target F1 during the target window. Figure 3a displays context and target preferences on the cortex of a single example patient. Among the electrodes that displayed target F1 selectivity, some also displayed selectivity for the context F1 during the context window (indicated with a black-and-white outline). Figure 3b displays the activation profile of one example electrode (e2). Importantly, e2 responds more strongly to low F1 targets during the target window (*sufu* preferent: $p = 2.4*10^{-21}$) but also to low F1 contexts during the context window (Speaker A

255 preferent: p= $1.7*10^{-14}$). This demonstrates that this neural population responded more strongly
256 to low F1 acoustic stimuli in general and is not exclusively selective for a discrete phoneme
257 category. Importantly, e2 also displayed normalization, as its activity was affected by context F1
258 during the *target* window (p = $2.7*10^{-4}$), and the direction of that context effect was consistent
259 with contrastive normalization (*cf*. Fig. 2d).

260 Extending this finding to the population of electrodes, we found a significant positive
261 correlation across all target-selective temporal lobe electrodes between an electrode's target
262 preference and its context preference (r = 0.64; p = $1.42*10^{-5}$; Figure 3c). Hence, neural
263 populations that are selective for target F1 in fact often displayed a more general preference to
264 specific F1 frequency ranges. Moreover, when restricting the test of normalization (assessed as
265 the correlation between target preferences and the context effect, as per Figure 2d) to those
266 electrodes that displayed significant selectivity for both target F1 and context F1, normalization
267 was again found (Figure S6). These findings confirm that normalization affects acoustic-
268 phonetic (i.e., pre-phonemic) representations of speech sounds in parabelt auditory cortex.
269

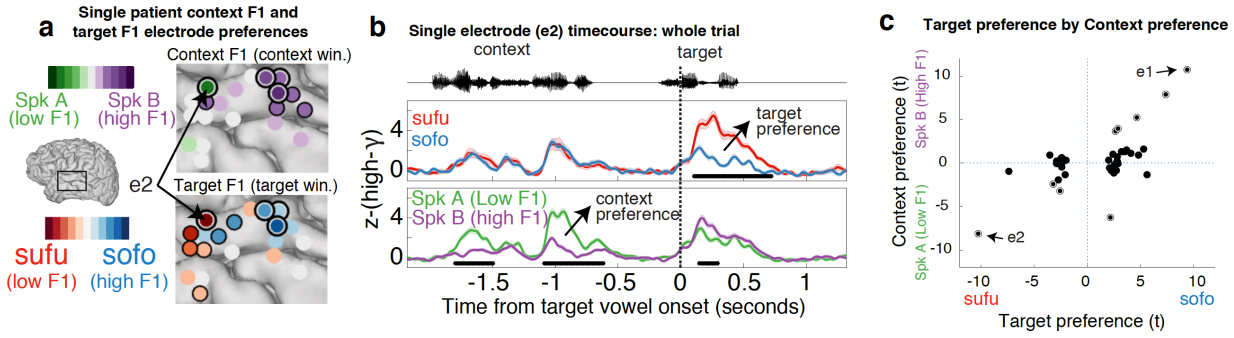

270

271 *Figure 3:* ***Sensitivity to contrast in acoustic-phonetic features****.* ***a****) Electrode preferences for*
272 *both target F1 (during target window) and context F1 (during context window) from a single*
273 *example patient. Some populations display both target F1 selectivity and context F1 selectivity*
274 *(marked with a black-and-white outline), indicating a preference for higher or lower F1 frequency*
275 *ranges. Others are only selective for target F1 or context F1 (marked with a single black outline*

in their respective panels). Significance assessed at p<0.05 uncorrected. ***b****) Mean (+/-1 SE) high-gamma activity at an example electrode (e2) from the example patient in panel a (conditions split as described in Fig 2c). Activity is displayed for a time window encompassing the full trial duration (both precursor sentence and target word). Black bars represent significant time points (p < 0.05; cluster-based permutation).* ***c****) A relation exists between the by-electrode context preference and target preference: electrodes that display a preference for either high or low target F1 typically also display a preference for the same F1 range during the context.*

Discussion

A critical challenge for human speech perception is the fact that different speakers produce the same speech sounds differently[1,3]. That is, speakers display different effective ranges with respect to their most informative speech cues (here, formants). We investigated the neural underpinnings of the behavioral finding that listeners rely on speaker-specific information to constrain phonetic processing. First, we observed behavioral normalization effects, replicating previous findings[7,8,10,11]. More importantly, analogous speaker-normalized representations of vowels were found in parabelt auditory cortex processing. These normalized representations were observed broadly across parabelt auditory cortex and were observed for all participants individually. Normalization was found to involve a context dependent change in the response strength of cortical populations that are selective for acoustic-phonetic features. These findings demonstrate that normalization is a highly robust phenomenon that results in a rescaling of representations that precede the mapping onto phonemes or higher level linguistic units.

Recent research has demonstrated that auditory cortex responds to the acoustic cues that are critical for both recognizing and discriminating phonemes[13–19] and different talkers[20–24] by means of different patterns of activation[37]. However, since cues that are critical for speaker and speech sound identification are conflated in the acoustic signal, these findings could be consistent either with a cortical representation of veridical acoustic properties

(e.g., reflecting the absolute F1 of a stimulus) or of context-dependent perceptual properties (e.g., its relative – or normalized – F1). Here, we were able to directly address the interaction between speaker and speech sound representations by presenting them to listeners at separate points in time and leveraging their immediate integration in auditory cortex processing. This approach demonstrated that rapid and broadly distributed normalization, or rescaling, is a basic principle of auditory cortex's encoding of speech sounds.

In behavioral research on normalization, the effect has often been discussed in relation to its contrastive nature. Indeed, we observed that a low F1 context led to more high F1 target percepts, which is consistent with an increase of perceptual contrast. Similar contrast enhancing operations have been widely documented in human and animal processing of various (nonspeech) acoustic stimuli[39–42], involving phenomena such as adaptive gain control[41] or stimulus specific adaptation[40,42]. An intuitive mechanism for the implementation of contrast enhancement involves sensory adaptation. This could be based on neuronal fatigue. When a neuron, or neuronal population, responds strongly to a masker stimulus, its response during a subsequent probe is often attenuated when the frequency of the probe falls within the neurons' excitatory receptive field[43,44]. But in addition to such local forms of adaptation, and possibly even more relevant for the effects observed here, adaptation also arises through (inhibitory) interactions between separate populations of neurons (which may have partly non-overlapping receptive fields)[39,41]. In the present study, spectral differences between the two context sentences and those between the endpoint target vowels were similar (see Figure S1). Adaptation may, hence, play a role in the type of normalization observed here. Indeed, we observed a number of populations for which a strong preference for one of the context sentences during the context window was associated with a decreased response during the target window (i.e., the normalization effect; Figure 3). Given the general nature of adaptation effects a relevant observation from the behavioral literature is the fact that various non-speech context sounds (e.g., broadband noise and musical tones) have also been observed to affect

the perception of speech sounds in a way that is at least qualitatively similar to those observed here[28,29,45]. This finding suggests that normalization effects may not be speech specific, and may, at least partly, be explained by adaptation effects.

An interesting additional question concerns the main locus of emergence of normalization. Broadly speaking, normalization could be inherited from primary auditory or subcortical processes (from which we were unable to record); it may largely emerge within parabelt auditory cortex processing itself; or it could be driven by top-down influences from regions outside of the auditory cortex. In our study, context and target sounds were separated in time by a 500ms silent interval. It has been suggested that adaptation effects over such longer latencies become especially dominant at cortical levels of processing[46,47]. Furthermore, behavioral experiments have demonstrated robust normalization effects with contralateral presentation of context and target sounds[28,45]. Both observations thus suggest that normalization can arise when the contribution of context effects that dominate peripheral auditory processing may be limited. With respect to the potential role of top-down modulations from regions outside of the auditory cortex, inferior frontal and sensorimotor cortex have been suggested to be involved in the resolving of perceptual ambiguities in speech perception[48,49] and could be expected to play a role in normalization too. Here we observed considerable activation in these regions, but they did not display normalization during the processing of the target sounds (see Figure S4). While tentative, these combined findings highlight the auditory cortex as the most likely locus for the emergence of normalization of speech sounds at this stage.

The current experiment involved data from cortical sites in both the left and right hemispheres. It has previously been demonstrated that the right hemisphere is more strongly involved in the processing of voice information[50,51]. Here, normalization was observed in left and right hemisphere patients (Figure 2f). Importantly, however, data included only two left

hemisphere and three right hemisphere patients in total, so no strong conclusions regarding lateralization can be drawn based on this dataset.

Despite broadly observed normalization of vowel representations, responses were not completely invariant to speaker differences during the context sentences (see for example the behavior of example electrode e2 in Figure 3b which displays a preference for the Low F1 sentence though most of the context window: i.e., it is not fully normalized). And indeed, our (and previous[8,9,28]) findings show that, even for target sound processing, surrounding contexts never results in *complete* normalization. While the F1 in the context sentences differed by roughly 400 Hz, the normalization effect only induces a shift of ~50 Hz in the position of the category boundaries (in behavior and in neural categorization). Normalization should thus be seen as a mechanism that biases processing in a context-dependent direction, but not one that fully constrains processing. Furthermore, context-based normalization is not the only means by which listeners tune-in to specific speakers. Listeners categorize sound continua differently when they are merely told they are listening to a man or a woman, demonstrating the existence of normalization mechanisms that do not rely on acoustic context[52]. In addition, formant frequencies are perceived in relation to other formants and pitch values in the current signal, because those features are correlated within speakers (e.g., people with long vocal tracts typically have lower pitch and lower formant frequencies overall). These “intrinsic” normalization mechanisms have been shown to affect auditory cortex processing of vowels as well[53–57]. Tuning-in to speakers in everyday listening is thus the result of the combination of at least these three distinct types of normalization[10].

To conclude, the results presented here reveal that the processing of vowels in auditory cortex becomes rapidly influenced by speaker-specific properties in preceding context. These findings add to recent literature that is ascribing a range of complex acoustic integration processes to the broader auditory cortex, suggesting that it participates in high-level encoding of speech sounds and auditory objects[14,25,58–60]. Recently, it has been demonstrated that

patches of parabelt auditory cortex represent speaker-invariant contours of intonation that speakers use to focus on one or the other part of a sentence[61]. The current findings build on these and demonstrate the emergence of speaker-normalized representations of acoustic-phonetic features and phonemes, the most fundamental building blocks of spoken language. This context-dependence allows auditory cortex to partly resolve the between-speaker variance present in speech signals. These features of auditory cortex processing underscore its critical role in our ability to understand speech in the complex and variable situations that we are exposed to every day.

Materials and Methods

Patients. A total of five human participants (2 male; all right handed; mean age 30.6 years), all native Spanish speaking (the US hospital at which participants were recruited has a considerable Spanish speaking patient population), were chronically implanted with high-density (256 electrodes; 4 mm pitch) multi-electrode cortical surface arrays as part of their clinical evaluation for epilepsy surgery. Arrays were implanted subdurally on the peri-Sylvian region of the lateral left (n = 2) or right (n = 3) hemispheres. Placement was determined by clinical indications only. All participants gave their written informed consent before the surgery, and had self-reported normal hearing. The study protocol was approved by the UC San Francisco Committee on Human Research. Electrode positions for reconstruction figures were extracted from tomography (CT) scans and co-registered with the patient's MRI.

Stimulus synthesis. Details of the synthesis procedure for these stimuli have been reported previously[8]. All synthesis was implemented in Praat software[62]. In brief, using source-filter separation, the formant tracks of multiple recordings of clear "sufu" and "sofo" were estimated. These estimates were used to calculate a single average time-varying formant track for both words, now representing an average of the formant properties over a number of instances of both [o] and [u]. The height of only the first formant of this filter model was increased and

405 decreased across the whole vowel to create the new formant models for the continuum from [u]
406 to [o] covering the distance between endpoints in 6 steps. These formant tracks were combined
407 with a model of the glottal-pulse source to synthesize the speech sound continuum. Synthesis
408 parameters thus dictated that all steps were equal in pitch contour, amplitude contour and had
409 identical contours for the formants higher than F1 (note that F1 and F2 values in Figure 1a and
410 S1 reflect measurements of the resulting sounds, not synthesis parameters). The two context
411 conditions were created through source-filter separation of a single spoken utterance of the
412 sentence “a veces se halla” (“at times she feels rather…”). The first formant of the filter model
413 was then increased or decreased by 100 Hz and recombined with the source model following
414 similar procedures as for the targets.
415 **Procedures.** The participants were asked to categorize the last words of a stimulus as either
416 “sufu” or “sofo”. Listeners responded using the two buttons on a button box. The two options
417 "sufu" and "sofo" were always displayed on the computer screen. Each of the 6 steps of the
418 continuum was presented in both the low- and high-F1 sentence conditions. Context conditions
419 were presented in separate mini-blocks of 24 trials (6 steps * 4 repetitions). Participants
420 participated in as many blocks as they felt comfortable with.
421 **Data acquisition and preprocessing.** Cortical Local Field Potentials (LFPs) were recorded
422 and amplified with a multichannel amplifier optically connected to a digital signal acquisition
423 system (Tucker-Davis Technologies) sampling at 3,052 Hz. The stimuli were presented
424 monaurally from loudspeakers at a comfortable level. The ambient audio (recorded with a
425 microphone aimed at the participant) along with a direct audio signal of stimulus presentation
426 were simultaneously recorded with the ECoG signals to allow for precise alignment and later
427 inspection of the experimental situation. Line noise (60Hz and harmonics at 120 and 180 Hz)
428 was removed from the ECoG signals with notch filters. Each time series was visually inspected
429 for excessive noise, and trials and or channels with excessive noise or epileptiform activity were
430 removed from further analysis. The remaining time series were common-average referenced

across rows of the 16x16 electrode grid. The time-varying analytic amplitude was extracted from eight bandpass filters (Gaussian, with logarithmically increasing center frequencies between 70–150 Hz, and semi-logarithmically increasing bandwidths) with the Hilbert transform. High-gamma power was calculated by averaging the analytic amplitude across these eight bands. The signal was subsequently down-sampled to 100Hz. The signal was z-scored based on the mean and standard deviation of a baseline period (from -50 to 0 ms before the onset of the context sentence) on a trial by trial basis. In the main text, high-γ will refer to this measure.

Single-electrode encoding analysis. We used ordinary least-squares linear regression to predict neural activity (high-γ) from our stimulus conditions (target F1 steps, coded as -2.5, -1.5, -0.5, 0.5, 1.5, 2.5; and context F1, coded as -1 and 1; as well as their interaction). These factors were used as numerical predictors to neural activity that was averaged across the target window (from 70 to 570 ms after target vowel onset) or across the context window (from 250 to 1450 ms after context sentence onset –a later onset was chose to reduce the influence of large and non-selective onset responses present in some electrodes-). For each model R-squared (Rsq) provides a measure of the proportion of variance in neural activity that is explained by the complete model. The p-value associated with the omnibus F-statistic provides a measure of significance. We set the significance threshold at alpha = 0.05 and corrected for multiple comparisons using the Bonferroni method, taking individual electrodes as independent samples. Figure S2a & b demonstrate that most of the variance in the context was explained by the factor context F1. During the target window however, both target F1 and context F1 explain a considerable portion of the variance. The interaction term was included to accommodate a situation where the context effect is more strongly expressed on one side of the target continuum than the other (see e.g., figure 2b, where the context effect is larger towards “sofo”), but is not further interpreted here.

For Figures 2d and Figure 3c, linear correlations between signed t-statistics of target F1 preferences and context effects (Figure 2d) or context preferences (Figure 3c) were computed

457 over all significant (9 [corrected] + 28 [uncorrected] = 37) electrodes. For Figure S6a, linear
458 correlations were computed separately for those electrodes that displayed significant selectivity
459 for Target F1 and Context F1 (n = 9; (marked with a black-and-white outline in S6a; r = -0.73; p
460 = 0.03), and for electrodes that displayed selectivity to Target F1 only (n = 28; S6a; r = -0.61; p
461 = $5.07*10^{-4}$). For Figure S6b the same approach was applied for each high-gamma sample
462 separately.
463 **Cluster-based permutation analyses.** For single example electrodes, a cluster-based
464 permutations approach was used to assess significance of differences between two event
465 related high gamma time courses (Figure 2c and Figure 3b; following the method described
466 in[63]). For each permutation, labels of individual trials were randomly assigned to data (high-y
467 time courses), and a t-test was performed for each timepoint. Next, for each time point (across
468 all 1000 permutations) a criterion value was established (the highest 95% of the [absolute] t-
469 values for that timepoint). Then, for each permutation, it was established when its value reached
470 above the criterion value and for how many samples it remained above criterion. A set of
471 subsequent timepoints above criterion is defined as a cluster. Then, for each cluster the t-values
472 were summed, and this value was assigned to that entire cluster. For each permutation only the
473 largest (i.e., highest summed cluster value) was stored as a single value. This resulted in a
474 distribution of maximally 1000 cluster values (some permutations may not result in any
475 significant cluster and have a summed t-value of 0). Then, using the same procedure, the size
476 of all potential clusters was established for the real data (correct assignment of labels), and it
477 was established whether the size of each cluster was larger than 95% of the permutation-based
478 cluster values. $p < 0.001$ indicates that the observed cluster was larger than all permutation
479 based clusters.
480 **Stimulus classification**. Linear Discriminant Analysis (LDA) models were trained to predict the
481 stimulus from the neural population responses evoked by the stimuli. Per participant a single
482 model was trained on all endpoint data, which was then used to predict labels for the ambiguous

items. To predict stimulus class for the endpoint stimuli (steps 1 and 6) a leave-one-out cross validation procedure was used to prevent overfitting. Model features (predictors) consisted of the selected timepoint*electrode combinations per participant.

For the analyses (Figures 2; Figure S3; Figure S4) training data consisted of high-y data averaged across a 500ms time window starting 70ms after target vowel onset (the target vowel was the first point of acoustic divergence between targets).

In the analyses, all task-related electrodes for a given participant (and region-of-interest, see Figure S4) were selected. Trial numbers per participant are listed in Table S1. The analysis displayed in Figure 2 and Figures S3 and S4 hence relied on a large number of predictors (electrodes * timepoints). While a large amount of predictors could result in overfitting, these parameters led to the highest proportion of correct classification for the endpoints (76% correct, see Figure S1b). High endpoint classification performance is important to establish the presence of normalization, but does not affect the extent of observed normalization, because the normalization effect is orthogonal. Importantly, in all analyses classification scores were only obtained from held-out data, preventing the fitting of idiosyncratic models. In addition, averaging across time (hence decreasing the number of predictors) led to qualitatively similar (and significant) effects for the important comparisons reported in this paper. Classification analyses resulted in a predicted class for each trial. These data were used as input for a generalized logistic linear mixed effects model.

Generalized Linear Mixed effects regression of classification data (glmer). For the analyses that assessed the effects of target stimulus F1 and context F1 on proportion of “sofo” responses (both behavioral and neural-classifier-based), the models had Target F1 (contrast coded, with the levels -2.5; -1.5; -0.5; 0.5; 1.5; 2.5) and Context F1 (levels -1; 1) entered as fixed effects, and uncorrelated by-patient slopes and intercepts for these factors as random effects.

For the analysis of the behavioral data, we observed more *sofo* responses towards the sofo end of the stimulus continuum ($B_{Target\ F1}$ = 1.89, z = 3.62, p < 0.001). Moreover, we observed an effect of context as items along the continuum were more often perceived as *sofo* (the vowel category corresponding to higher F1 values) after a low F1 voice (Speaker A) than after a high F1 voice (Speaker B) ($B_{Context\ F1}$ = -1.71, *z* = -3.15, p = 0.002).

For the analyses of neural representations the dependent variable consisted of the classes predicted by LDA stimulus classification described above. For the overall analysis including temporal lobe electrodes, the model revealed significant classification of the continuum ($B_{Target\ F1}$ = 0.50, *z* = 13.18, p < 0.001), suggesting reliable neural differences between the endpoints. Furthermore, an effect was also found for the factor Context on the proportion of "sofo" classifications ($B_{Context\ F1}$ = -0.28, *z* = -4.67, p < 0.001), reflecting the normalization effect of most interest. For the analysis focusing on the dorsal and frontal electrodes a significant effect of Step was observed, that is, significant classification of the continuum ($B_{Target\ F1}$ =0.20, *z* = 6.04, p< 0.001), but no significant influence of context ($B_{Context\ F1}$ = 0.02, *z* = 0.31 p = 0.76) see S4C for further detail.

Multidimensional scaling. The neural dissimilarity between all 12 pairs of target items was measured by computing leave-one-out LDA classification scores between each target pair. Here, a high classification score reflects different neural representations, a low score reflects similarity. The resulting 12*12 dissimilarity matrices were averaged across participants (Figure S5a). The across-participant average of the classification-based distance matrices was projected in Multidimensional Scaling space. The first (i.e., main) dimension reflected stimulus step (see Figure S5b), indicating that this is indeed the most dominant property of the selected electrode population. Importantly, this dimension also reflected normalization

Author Contributions

M.J.S. and K.J., conceived the study. M.J.S. designed the experiments, generated the stimuli and analyzed the data. M.J.S., N.F. and E.F.C. collected the data. M.J.S. and N.F. interpreted the data and wrote the manuscript. M.J.S., N.F., K.J., and E.F.C. edited the manuscript.

Code availability.

These results were generated using code written in Matlab. Code will be publicly available through the Open Science Framework osf.io/u7xnp.

Data availability.

The data that support the findings of this study will be publicly available through the Open Science Framework osf.io/u7xnp.

Competing interests.

The authors declare no competing interests.

Acknowledgements.

We are grateful to Matthew Leonard for commenting on an earlier version of this manuscript. This work was supported by European Commission grant FP7-623072 (MJS); and NIH grants F32-DC013486, R00-NS065120, DP2-OD00862, and R01-DC012379 (E.F.C.); and F32DC015966 (N.P.F.).

References

1. Liberman AM, Cooper FS, Shankweiler DP, Studdert-Kennedy M. Perception of the speech code. Psychol Rev. 1967;74(6):431–61.
2. Diehl RL, Lotto AJ, Holt LL. Speech perception. Annu Rev Psychol. 2004;55:149–79.
3. Peterson GE, Barney HL. Control methods used in a study of the vowels. Jounal Acoust

559 Soc Am. 1952;24(2):175–84.

560 4. Newman RS, Clouse SA, Burnham JL. The perceptual consequences of within-talker
561 variability in fricative production. J Acoust Soc Am. 2001;109(3):1181–96.

562 5. Chodroff E, Wilson C. Structure in talker-specific phonetic realization: Covariation of stop
563 consonant VOT in American English. J Phon. 2017;61:30–47.

564 6. Ladefoged P, Johnson K. A course in phonetics. Nelson Education; 2014.

565 7. Ladefoged P, Broadbent DE. Information Conveyed by Vowels. J Acoust Soc Am.
566 1957;29(1):98–104.

567 8. Sjerps MJ, Smiljanić R. Compensation for vocal tract characteristics across native and
568 non-native languages. J Phon. 2013;41(3–4):145–55.

569 9. Johnson K. Speaker Normalization in Speech Perception. Handb Speech Percept.
570 2005;(Figure 1):363–89.

571 10. Nearey TM. Static, dynamic, and relational properties in vowel perception. J Acoust Soc
572 Am. 1989;85(5):2088–113.

573 11. Sjerps MJ, Zhang C, Peng G. Lexical Tone is Perceived Relative to Locally Surrounding
574 Context, Vowel Quality to Preceding Context. J Exp Psychol Hum Percept Perform. 2017;

575 12. Ladefoged P. A note on '"Information conveyed by vowels."' J Acoust Soc Am.
576 1989;85(5):2223–4.

577 13. Creutzfeldt O, Ojemann GA, Lettich E. Neuronal activity in the human lateral temporal
578 lobe: I. Responses to Speech. Exp Brain Res. 1989;77:451–75.

579 14. Chang EF, Rieger JW, Johnson K, Berger MS, Barbaro NM, Knight RT. Categorical
580 speech representation in human superior temporal gyrus. Nat Neurosci. 2010 Nov
581 3;13(11):1428–32.

582 15. Hickok G, Poeppel D. Neural basis of speech perception. Hum Audit Syst Fundam Organ
583 Clin Disord. 2015;129:149–60.

584 16. Hickok G, Poeppel D. The cortical organization of speech processing. Nat Rev Neurosci.

2007;8(5):393–402.

17. Boatman D, Lesser RP, Gordon B. Auditory speech processing in the left temporal lobe: An electrical interference study. Vol. 51, Brain and Language. 1995. p. 269–90.

18. Scott SK, Johnsrude IS. The neuroanatomical and functional organization of speech perception. Trends Neurosci. 2003;26(2):100–7.

19. Steinschneider M, Nourski K V., Kawasaki H, Oya H, Brugge JF, Howard MA. Intracranial study of speech-elicited activity on the human posterolateral superior temporal gyrus. Cereb Cortex. 2011;21(10):2332–47.

20. Andics A, McQueen JM, Petersson KM. Mean-based neural coding of voices. Neuroimage. 2013;79:351–60.

21. Andics A, McQueen JM, Petersson KM, Gál V, Rudas G, Vidnyánszky Z. Neural mechanisms for voice recognition. Neuroimage. 2010;52(4):1528–40.

22. Belin P, Zatorre RJ, Lafaille P, Ahad P, Pike B. Voice-selective areas in human auditory cortex. Nature. 2000;403(6767):309–12.

23. Kriegstein K von, Kleinschmidt A, Sterzer P, Giraud A-L. Interaction of Face and Voice Areas during Speaker Recognition. J Cogn Neurosci. 2005;17(3):367–76.

24. Von Kriegstein K, Giraud AL. Distinct functional substrates along the right superior temporal sulcus for the processing of voices. Neuroimage. 2004;22(2):948–55.

25. Mesgarani N, Cheung C, Johnson K, Chang EF. Phonetic Feature Encoding in Human Superior Temporal Gyrus. Science (80-). 2014;343(6174):1006–10.

26. Pasley BN, David S V., Mesgarani N, Flinker A, Shamma SA, Crone NE, et al. Reconstructing Speech from Human Auditory Cortex. PLoS Biol. 2012;10(1):e1001251.

27. Kluender KR, Coady JA, Kiefte M. Sensitivity to change in perception of speech. Speech Commun. 2003;41(1):59–69.

28. Watkins AJ. Central, auditory mechanisms of perceptual compensation for spectral-envelope distortion. J Acoust Soc Am. 1991;90(6):2942–55.

611 29. Stilp CE, Alexander JM, Kiefte M, Kluender KR. Auditory color constancy: Calibration to
612 reliable spectral properties across nonspeech context and targets. Atten Percept
613 Psychophys. 2010;72(2):470–80.
614 30. Sjerps MJ, Mitterer H, McQueen JM. Hemispheric differences in the effects of context on
615 vowel perception. Brain Lang. 2012;120(3).
616 31. Goldinger SD. Echoes of Echoes? An Episodic Theory of Lexical Access. Psychol Rev.
617 1998;105(2):251–79.
618 32. Leonard MK, Chang EF. Dynamic speech representations in the human temporal lobe.
619 Trends Cogn Sci. 2014;18(9):472–9.
620 33. Nourski K V., Steinschneider M, Rhone AE, Oya H, Kawasaki H, Howard MA, et al.
621 Sound identification in human auditory cortex: Differential contribution of local field
622 potentials and high gamma power as revealed by direct intracranial recordings. Brain
623 Lang. 2015;148:37–50.
624 34. Steinschneider M, Fishman YI, Arezzo JC. Spectrotemporal analysis of evoked and
625 induced electroencephalographic responses in primary auditory cortex (A1) of the awake
626 monkey. Cereb Cortex. 2008;18(3):610–25.
627 35. Ray S, Maunsell JHR. Different origins of gamma rhythm and high-gamma activity in
628 macaque visual cortex. PLoS Biol. 2011;9(4).
629 36. Crone N, Crone N, Boatman D, Boatman D, Gordon B, Gordon B, et al. Induced
630 electrocorticographic gamma activity during auditory perception. Clin Neurophysiol.
631 2001;112:565–82.
632 37. Formisano E, De Martino F, Bonte M, Goebel R. “Who” Is Saying “What”? Brain-Based
633 Decoding of Human Voice and Speech. Science (80-). 2008;322(5903):970–3.
634 38. Chan AM, Dykstra AR, Jayaram V, Leonard MK, Travis KE, Gygi B, et al. Speech-specific
635 tuning of neurons in human superior temporal gyrus. Cereb Cortex. 2014;24(10):2679–
636 93.

637 39. Brosch M, Schreiner CE. Time course of forward masking tuning curves in cat primary
638 auditory cortex. J Neurophysiol. 1997;77(2):923–43.
639 40. Ulanovsky N, Las L, Farkas D, Nelken I. Multiple Time Scales of Adaptation in Auditory
640 Cortex Neurons. J Neurosci. 2004 Nov 17;24(46):10440–53.
641 41. Rabinowitz NC, Willmore BDB, Schnupp JWH, King AJ. Contrast Gain Control in Auditory
642 Cortex. Neuron. 2011;70(6):1178–91.
643 42. Pérez-González D, Malmierca MS. Adaptation in the auditory system: an overview. Front
644 Integr Neurosci. 2014;8(February):1–10.
645 43. Harris DM, Dallos P. Forward masking of auditory nerve fiber responses. J Neurophysiol.
646 1979;42(4):1083–107.
647 44. Smith RL. Short-term adaptation in single auditory nerve fibers: some poststimulatory
648 effects. J Neurophysiol. 1977;40(5):1098–111.
649 45. Sjerps MJ, Mitterer H, McQueen JM. Hemispheric differences in the effects of context on
650 vowel perception. Brain Lang. 2012;120(3):401–5.
651 46. Phillips EAK, Schreiner CE, Hasenstaub AR. Cortical Interneurons Differentially Regulate
652 the Effects of Acoustic Context. Cell Rep. 2017;20(4):771–8.
653 47. Fitzpatrick DC, Kuwada S, Kim DO, Parham K, Batra R. Responses of neurons to click-
654 pairs as simulated echoes: auditory nerve to auditory cortex. J Acoust Soc Am.
655 1999;106(6):3460–72.
656 48. Pulvermuller F, Huss M, Kherif F, Moscoso del Prado Martin F, Hauk O, Shtyrov Y. Motor
657 cortex maps articulatory features of speech sounds. Proc Natl Acad Sci.
658 2006;103(20):7865–70.
659 49. Wilson SM, Iacoboni M. Neural responses to non-native phonemes varying in
660 producibility: Evidence for the sensorimotor nature of speech perception. Neuroimage.
661 2006;33(1):316–25.
662 50. Myers EB, Theodore RM. Voice-sensitive brain networks encode talker-specific phonetic

663 detail. Brain Lang. 2017;165:33–44.

664 51. Belin P, Zatorre RJ. Adaptation to speaker ' s voice in right anterior temporal lobe.
665 Neuroreport. 2003;14(16):2105–9.

666 52. Johnson K, Strand EA, D'Imperio M. Auditory-visual integration of talker gender in vowel
667 perception. J Phon. 1999;27(4):359–84.

668 53. Edmonds BA, James RE, Utev A, Vestergaard MD, Patterson RD, Krumbholz K.
669 Evidence for early specialized processing of speech formant information in anterior and
670 posterior human auditory cortex. Eur J Neurosci. 2010;32(4):684–92.

671 54. Andermann M, Patterson RD, Vogt C, Winterstetter L, Rupp A. Neuromagnetic correlates
672 of voice pitch, vowel type, and speaker size in auditory cortex. Neuroimage.
673 2017;158(February):79–89.

674 55. Monahan PJ, Idsardi WJ. Auditory sensitivity to formant ratios: Toward an account of
675 vowel normalisation. Lang Cogn Process. 2010;25(6):808–39.

676 56. Kreitewolf J, Gaudrain E, von Kriegstein K. A neural mechanism for recognizing speech
677 spoken by different speakers. Neuroimage. 2014;91:375–85.

678 57. von Kriegstein K, Smith DRR, Patterson RD, Kiebel SJ, Griffiths TD. How the Human
679 Brain Recognizes Speech in the Context of Changing Speakers. J Neurosci.
680 2010;30(2):629–38.

681 58. Engineer CT, Perez C a, Chen YH, Carraway RS, Reed AC, Shetake J a, et al. Cortical
682 activity patterns predict speech discrimination ability. Nat Neurosci. 2008 May [cited 2013
683 Mar 7];11(5):603–8.

684 59. Leonard MK, Baud MO, Sjerps MJ, Chang EF. Perceptual restoration of masked speech
685 in human cortex. Nat Commun. 2016;7:13619.

686 60. Bizley JK, Walker KMM, Nodal FR, King AJ, Schnupp JWH. Auditory cortex represents
687 both pitch judgments and the corresponding acoustic cues. Curr Biol. 2013;23(7):620–5.

688 61. Tang C, Hamilton LS, Chang EF. Intonational speech prosody encoding in the human

auditory cortex. Science. 2017;357(6353):797–801.

62. Boersma P, Weenink D. Praat: Doing phonetics by computer (Version 5.1). 2009.

63. Maris E, Oostenveld R. Nonparametric statistical testing of EEG- and MEG-data. J Neurosci Methods. 2007;164(1):177–90.

Supporting information:

S1:

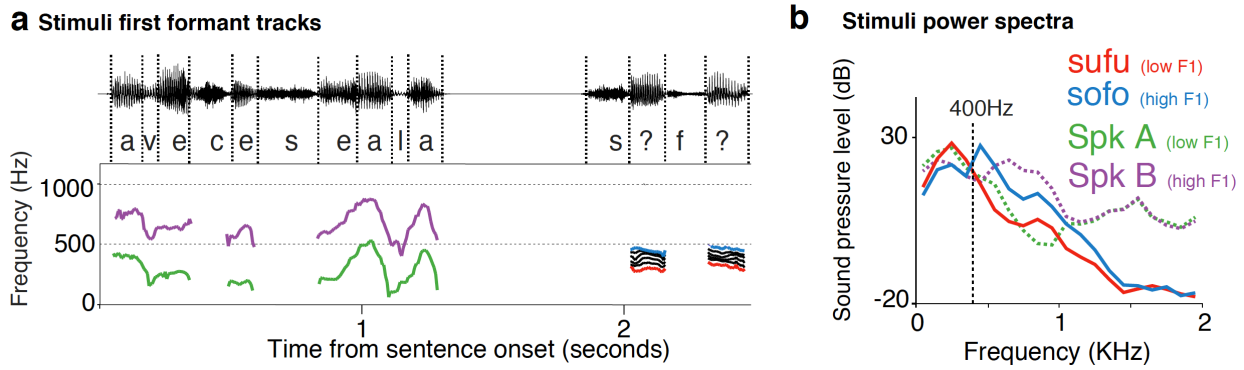

Figure S1: ***Contexts and targets display similar spectral differences****.* ***a****) First formant tracks for the voiced portions of the synthesized materials. In the annotation "?" indicates one of the target vowel steps.* ***b)*** *A similar spectral relation exists between the two endpoint targets /u/ vs. /o/ and the context sentences. /u/ and the low F1 speaker have more dominant low frequency components (i.e., below 400 Hz) in the spectrum than /o/ and the High F1 speaker.*

707 S2:

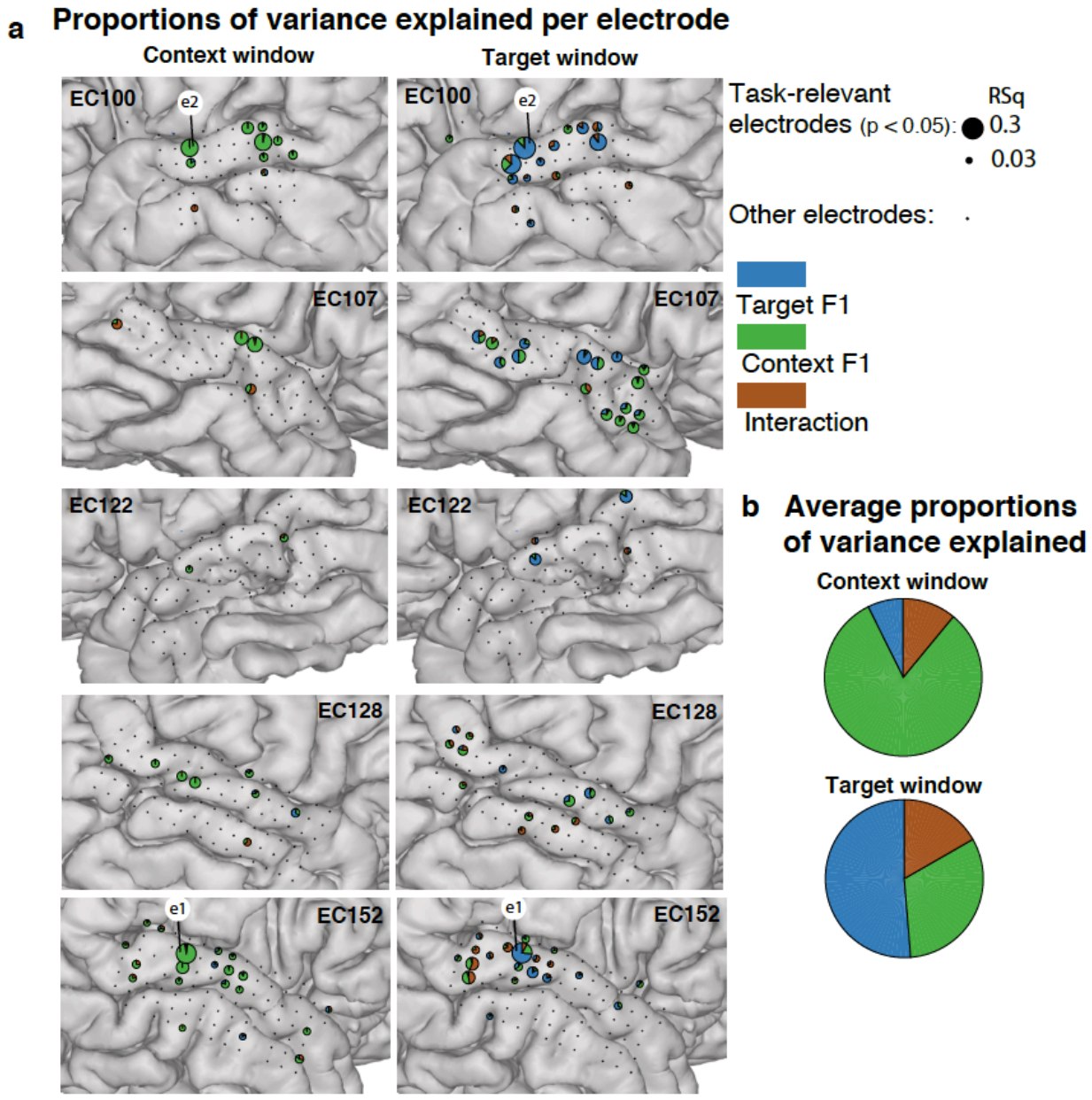

708

709 *Figure S2:* ***Context F1 influences cortical activity during target processing. a****) Map of*

710 *context and target encoding for all task-related electrodes of all subjects (temporal lobe only),*

711 *both during the context window (left column) and during the target window (right column). The*

712 *areas of the pie-charts are proportional to the total variance explained. Wedges show the*

713 *relative variance explained by each factor (stimulus dimension) for each significant electrode.* ***b****)*

Weighted average proportion of variance explained by main effects and interactions across all significant electrodes (across all 5 patients). During the context window, context properties explain the large majority of variance. During the target window, the context stimulus properties still explain a considerable portion of the variance.

719 S3:

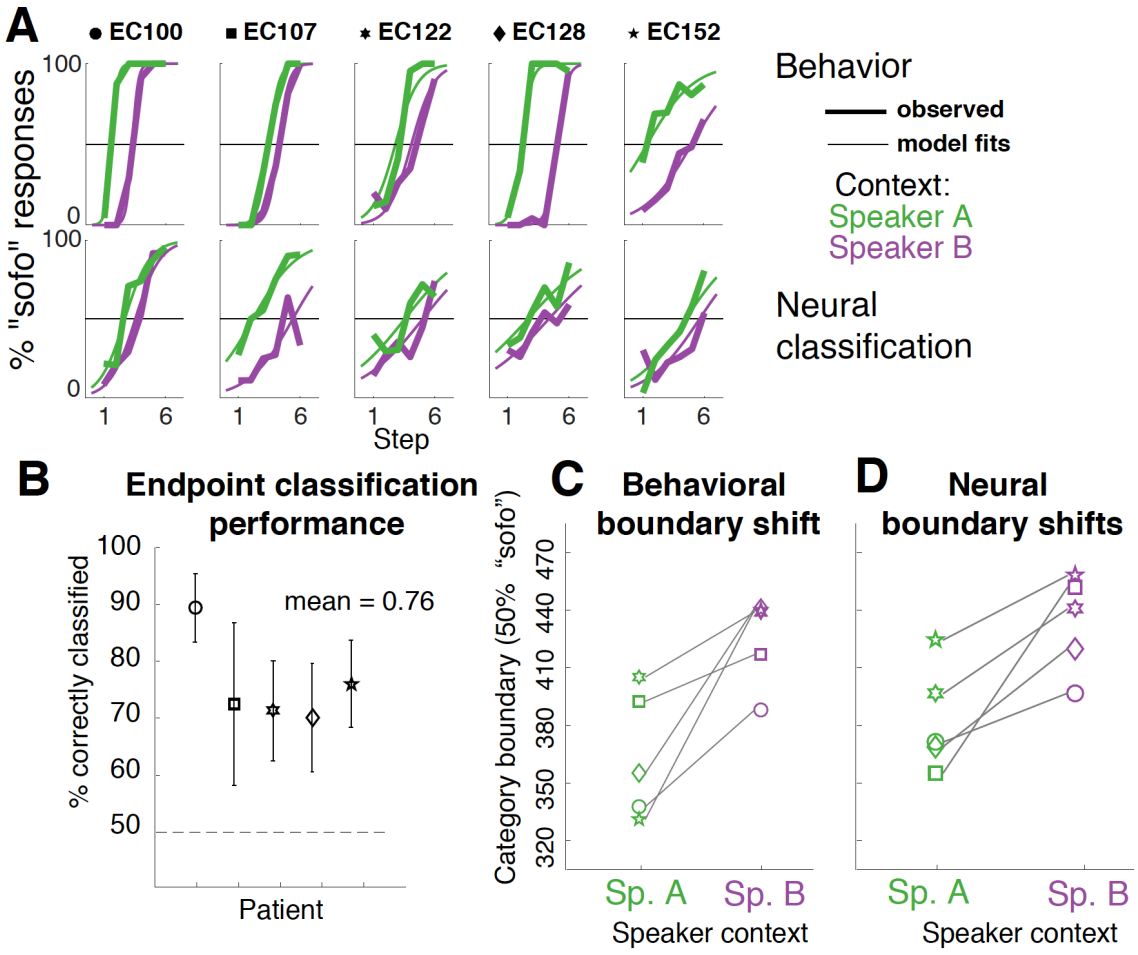

720

721 *Figure S3:* ***All participants display context effects in both their behavior and neural***

722 ***responses****.* ***a****) Top row: Observed mean proportions of "sofo" responses across the steps of the*

723 *continuum in both context conditions for all participants (thick lines). Model fits (thin lines) are*

724 *used to estimate the 50% category boundary per condition per participant (used for panel c).*

725 *Bottom: same as in top panel but for the neural classification data (thick lines reflect LDA-based*

726 *predictions).* ***b****) overall percentage correct (leave-one-out) classification on the endpoints per*

727 *participant (with bootstrapped 95% CI).* ***c****) By-participant indications of the estimated 50%*

728 *category boundaries in the two context conditions based on behavior.* ***d****) same as c but for 50%*

729 *category boundary estimates of the neurally-based classification (i.e., identical to Figure 2d, but*

730 *reproduced for comparison to Fig. S3c).*

731 S4:

732

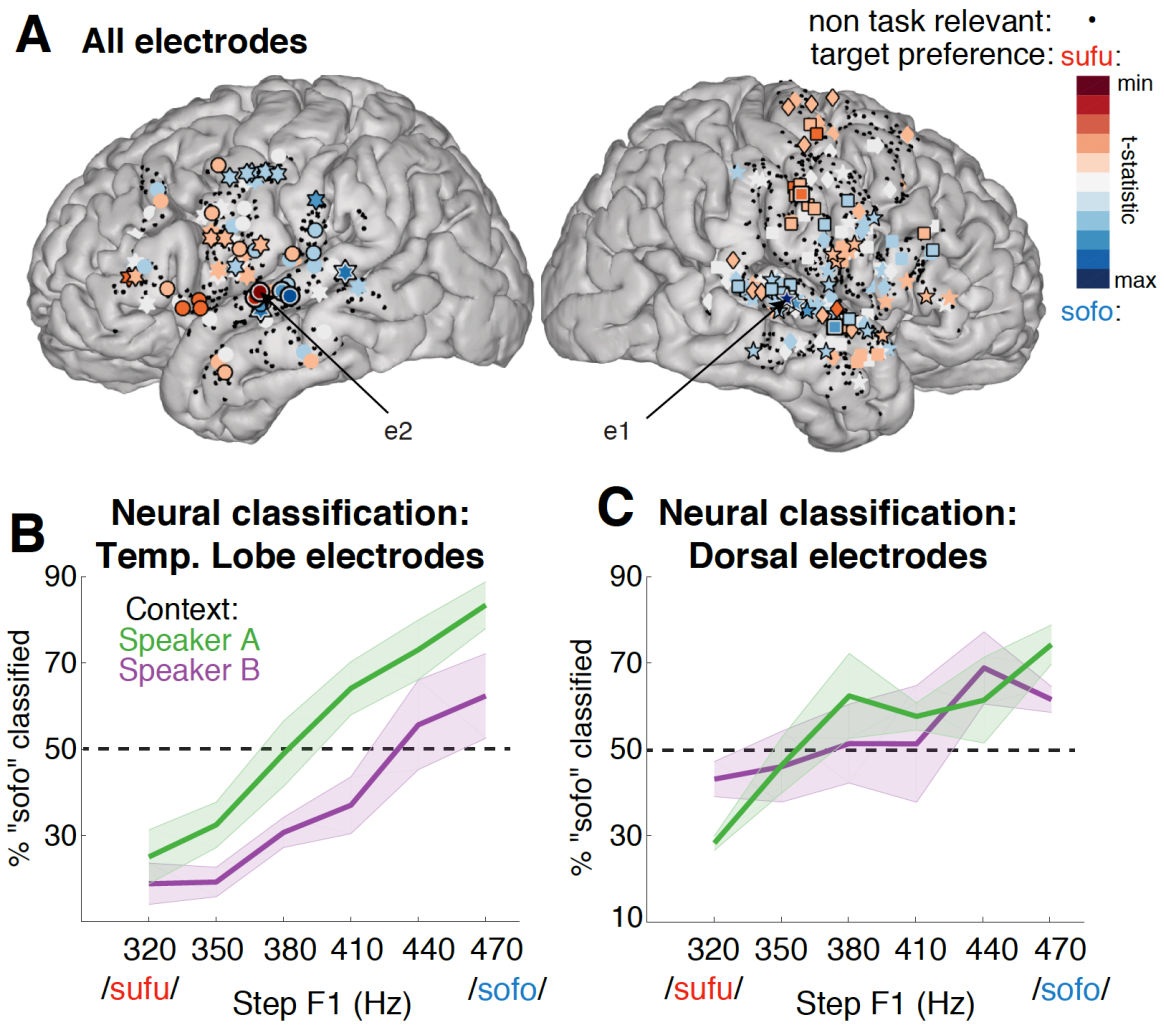

733

734 *Figure S4:* ***Normalization is observed only in temporal lobe regions a****) Target vowel*

735 *selective electrodes are congregated on the temporal lobe, although some are also found in*

736 *frontal regions.* ***b****) when including temporal electrodes, LDA classification results (averaged*

737 *across participants) reveal a strong context effect.* ***c****) no context effect is observed for LDA*

738 *classification results based on electrodes from dorsal (i.e., all non-temporal) regions.*

739

740

741

742 S5:

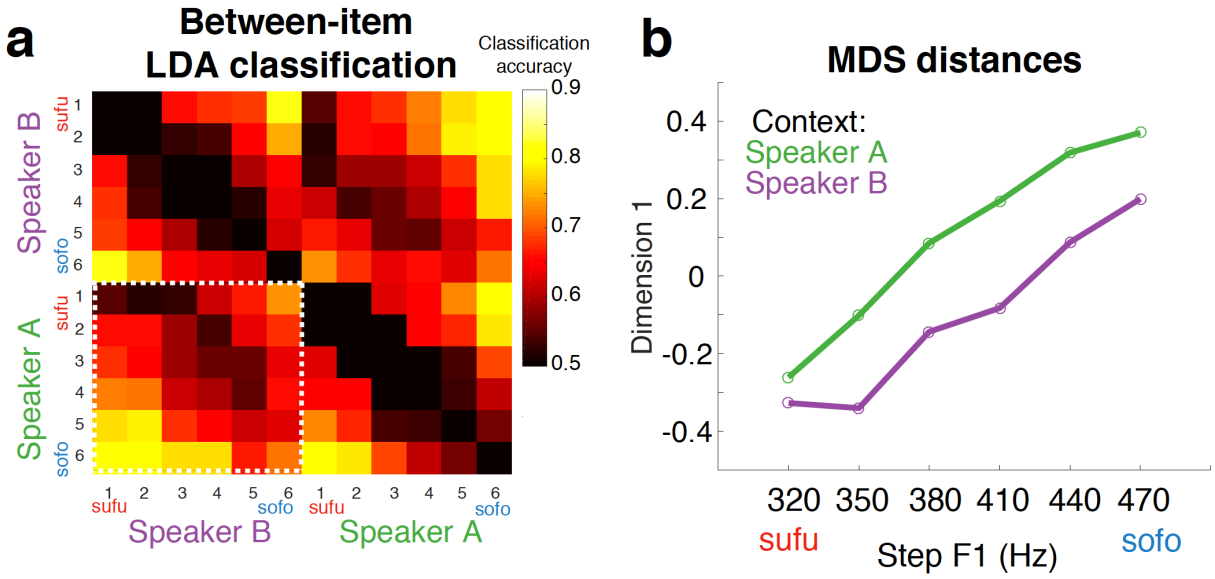

743

744 *Figure S5:* ***Between stimulus neural distances reflect normalization a)*** *Distance matrix*
745 *based on between-stimulus leave-one-out LDA classification of a two-class classifier. High*
746 *classification performance reflects large neural distances. The lower left corner (involving the*
747 *between-context comparisons; marked with a white-dashed outline) demonstrates*
748 *normalization: e.g., step 2 of Speaker A is most similar to step 4 of Speaker B, etc. Under*
749 *veridical processing, smallest distances would follow the sub-diagonal (with the smallest*
750 *distances for the comparisons of 1 vs. 1; 2 vs. 2; etc.)* ***b)*** *Multidimensional scaling (MDS) based*
751 *on the distance matrix (in a) reveals that target stimulus F1 is the main factor (D1) determining*
752 *neural dissimilarity. Critically, this dimension is also influenced by context F1. That is, it reflects*
753 *normalization.*

754

S6

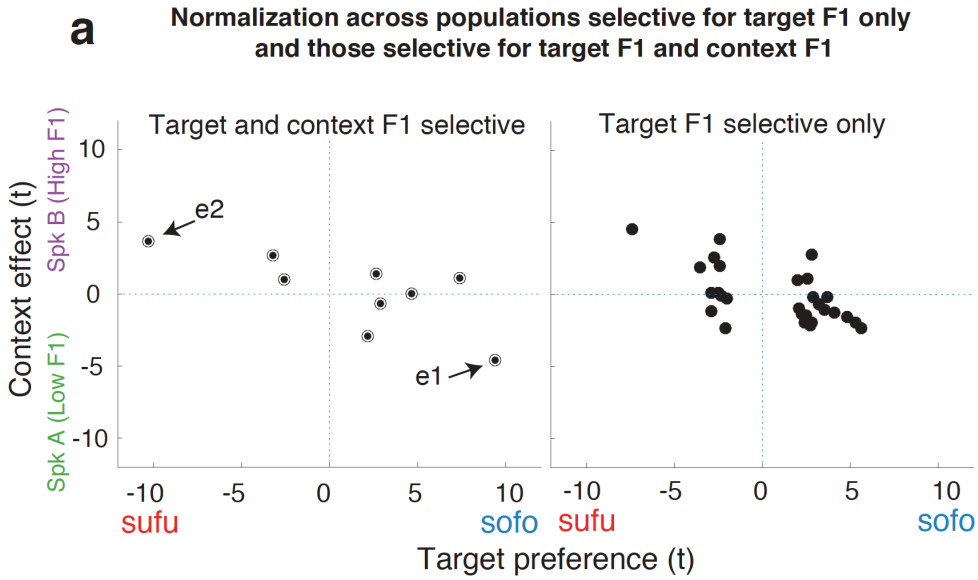

Figure S6: ***Normalization across target F1 selective population types****. Panels displays the same relation as Figure 2d, (the relation between target preference and context effect; i.e., normalization), but for two types of populations. Normalization is observed for electrodes that are most clearly selective for acoustic-phonetic features (instead of phonemes) since they display preferences for both target F1 and context F1 (left panel; black-and-white outline; target and context materials contain different phonemes). For completeness; normalization is also observed for those electrodes that display target F1 preferences only (right panel; black fill). See Figure 3 for reference.*

SUPPLEMENTARY TABLES

S1: **Trial counts**

Item	EC100	EC107	EC122	EC128	EC152
High_1	24	9	28	23	33
High_2	24	9	26	23	26
High_3	24	12	31	24	31
High_4	23	11	27	24	27
High_5	24	11	29	19	29
High_6	24	9	27	22	26
Low_1	23	11	25	21	31
Low_2	24	12	27	21	29
Low_3	24	9	23	20	33
Low_4	23	8	30	20	31
Low_5	24	10	25	19	31
Low_6	23	11	28	21	31

S2: **Electrode type counts** (temporal lobe)

Patient	Task-related	Target F1(corrected)	Context F1(corrected)
EC100	21	10(4)	8(3)
EC107	19	7(1)	4(2)
EC122	6	3(2)	3(0)
EC128	20	6(0)	10(2)
EC152	32	11(2)	16(4)